



### Science Arts & Métiers (SAM)

is an open access repository that collects the work of Arts et Métiers Institute of Technology researchers and makes it freely available over the web where possible.

This is an author-deposited version published in: <https://sam.ensam.eu>  
Handle ID: <http://hdl.handle.net/10985/19787>

#### To cite this version :

Bertrand MARCON, Jean-Claude BUTAUD, Louis DENAUD, Robert COLLET, Joffrey VIGUIER -  
Panel Shear of Plywood in Structural Sizes - Assessment Improvement Using Digital Image  
Correlation - Experimental Techniques p.0 - 2021

Any correspondence concerning this service should be sent to the repository

Administrator : [scienceouverte@ensam.eu](mailto:scienceouverte@ensam.eu)





# Panel Shear of Plywood in Structural Sizes - Assessment Improvement Using Digital Image Correlation

J. Viguier<sup>1</sup> · B. Marcon<sup>1</sup> · J. C. Butaud<sup>1</sup> · L. Denaud<sup>1</sup> · R. Collet<sup>1</sup>

Received: 25 June 2019 / Accepted: 8 December 2020  
 © Springer Nature Switzerland AG part of Springer Nature 2020

## Abstract

This paper introduces a new test configuration for the determination of panel shear properties in structural sizes. This original test configuration has been successfully applied to calculate the shear properties of beech plywood. A numerical model has been developed to evaluate the influence of such a novel setup in comparison to the common standard. The research includes the mechanical characterization of a total of 36 samples using Digital Image Correlation (DIC) to measure the in plane displacements. The use of DIC has been proven to be efficient to measure the shear properties and also acts as a tool to ensure that the sollicitation was adequate during the test. Finally, the results highlight the interest to actually perform the proposed test instead of using the alternative density-based equivalencies provided by the standards.

**Keywords** Shear · DIC · Beech · Plywood

## Introduction

Plywood is often used in the construction sector. In particular, high quality beech plywood could exhibit great features to be used in the construction for plywood gussets in nailed or glued trusses or as a web of I-Joist. Therefore obtaining reliable shear properties for plywood is essential to ensure security and cost efficiency in the legal range of the building standards. The measured shear properties has not been found to be a constant value [1], but appears to be affected by the method of shear properties determination even when controlling all factors which normally affect the mechanical properties of wood. The evaluation of shear properties has conducted to create a wide range of standardized and non-standardized test methods (two rails, plate shear, bending tests, torsion, ...). Among those, the two rails type seems to be preferred in order to test plywood in structural size. During this test, the load is transferred to the specimen through two pair of rails glued or bolted parallel to its longer edge in such a way that the shear is nearly pure in the central area. Several studies [2–6] have

been conducted over the years to develop or assessing the difference between two-rails type tests.

The area exposed to shear has been kept nearly constant over the years to a rectangle of approximately 200 by 600 mm<sup>2</sup>. Different strategies to perform this test have been experienced, all of them requiring complicated apparatus (see Fig. 1). In the latest European standard (EN 789 [7]), this area has been changed to a more complicated shape with a slightly lower area (see Fig. 1(c)) but the principle and the complexity remain constant. This complexity probably causes the lack of values issued from plywood performance declaration of the majority of the plywood panel manufacturers. Indeed, the producers prefer to use density equivalencies given in EN 12369-2 [8] to provide shear properties even if they are very penalizing and do not reflect the true mechanical properties of plywood panels especially in the case of beech.

Panels shear modulus is usually measured using a Linear Variable Differential Transformer (LVDT) orientated by 45° across the central area (symbolized by a rectangle in Fig. 1) on each side of the specimen and then averaged. Timbers shear modulus can also be determined through flexural [9] or torsional [10] vibration mechanical tests with accelerometers and more or less complex finite elements analysis (FEA). In this study, Digital Image Correlation (DIC) is proposed as an alternative to the fixation of LVDT and as a substantial improvement to measure those displacements. In the past 30 years, DIC has proved to be

✉ J. Viguier  
 joffrey.viguier@gmail.com

<sup>1</sup> LaBoMaP, Arts et Metiers Institute of Technology, LaBoMaP, HESAM Université, rue Porte de Paris, F-71250, Cluny, France



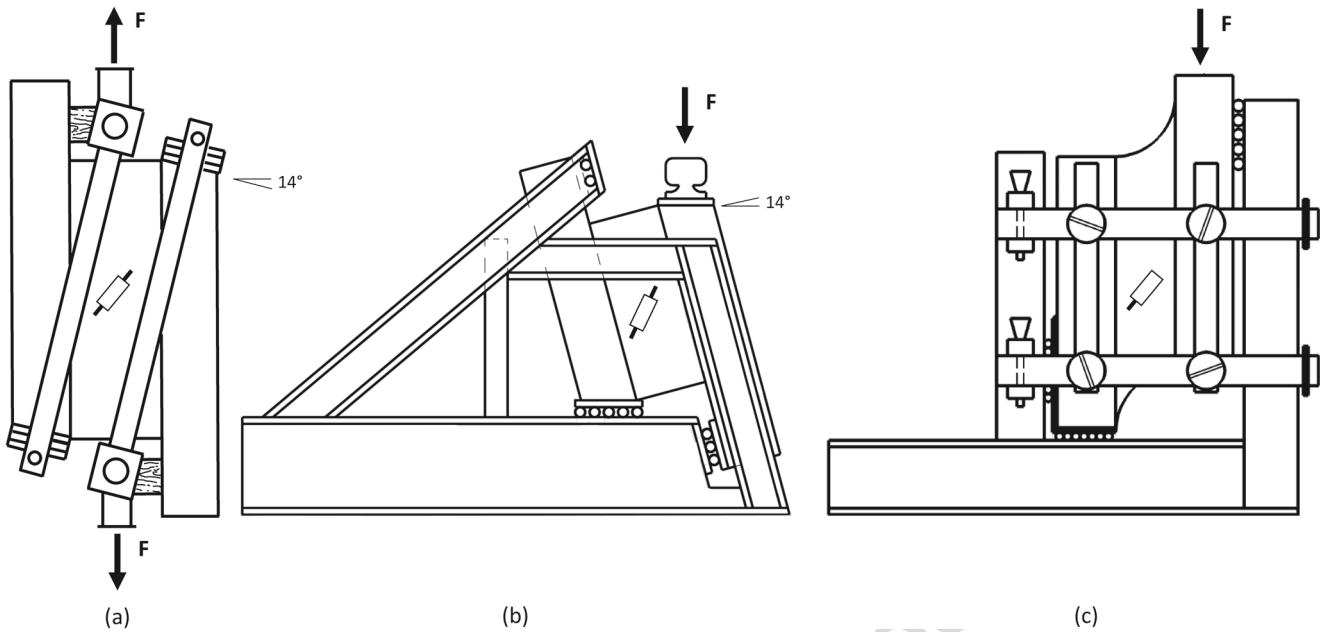


**Fig. 1** Different two-rails configuration tests used or in use within the past 30 years

48 a very valuable non-invasive tool for full-field displacement  
 49 measurements [11–14] and its accuracy has been proven  
 50 [15]. The use of DIC in the field of wood testing is  
 51 increasing [16–18].

52 The main objective of the present study is to propose a  
 53 simpler method to determine the shear properties of wooden  
 54 panels and more particularly plywood ones. In addition an  
 55 experimental part designed to validate the modified test  
 56 using full field measurements, finite elements numerical  
 57 simulations have been used to determine the influence of  
 58 using the proposed test method on the mechanical properties  
 59 of the plywood panels.

60 **Materials and Methods**

61 **Sampling**

62 A total of 18 beech plywood panels were used for this  
 63 study and two different thicknesses (18 and 25 mm with  
 64 respectively 9 and 11 plies) have been studied. Samples  
 65 were cut using a three-axis router machine according to  
 66 the shape described in Fig. 2. In order to define a test  
 67 which can be performed easier than the one described in  
 68 the standard [7], involving a less bulky setup, the chosen  
 69 strategy was to tilt the sample. For the experimental part,  
 70 the angle  $\alpha$  has been taken equal to  $18^\circ$  in such a way  
 71 that the moment is nearly equal to 0. In doing so, the  
 72 special apparatus described in the standard was not needed  
 73 anymore and the initially complex test looks like a simple  
 74 self balanced compression test. Four Douglas-fir timber

rails with a thickness equals to 35 mm have then been glued  
 using polyvinyl acetate (PVAC) to each specimen to avoid  
 buckling of the sample during the test as required by the  
 standard [7]. Two samples have been cut from each panel  
 : one having its external ply with fiber along the longest  
 dimension and the second one perpendicular to its longest  
 dimension. Finally, 36 samples have been made.

82 **Mechanical Test and Displacements Measurement**

83 The tests were performed with a Zwick Roell static material  
 84 testing machine with a 250 kN load cell. The load was  
 85 applied on the top surface of the timber rails with an  
 86 adjusted application rate, so that the maximum load was  
 87 reached within  $300 \pm 120$  s according to EN 789 [7].  
 88 In practice, the loading rate has been chosen equals to 2  
 89 mm/min. The shear deformation was measured on both  
 90 faces in the middle of the specimen using 2D digital image  
 91 correlation. Images of both faces and their corresponding  
 92 load were recorded during the whole test. Digital frames  
 93 of both sides of the specimen were recorded using two  
 94 Basler ace acA1920-155um type imagers equipped with  
 95 Pentax Ricoh FL-CC3516-2M - 1.6 / 35 mm lenses. Those  
 96 cameras exhibit a resolution of 1920 by 1200 square pixels  
 97 with a pitch size of  $5.86e^{-3}$  mm<sup>2</sup>. The observed area was  
 98 set to 211 by 132 mm<sup>2</sup> thanks to extension tubes with a  
 99 working distance (standoff distance) of 1 meter. The scene  
 100 was illuminated using identical white LED projectors on  
 101 both sides and a built-in lens diaphragm used to reach  
 102 identical grey level repartition histograms for both sides of  
 103 the specimen. The geometrical centres had been marked

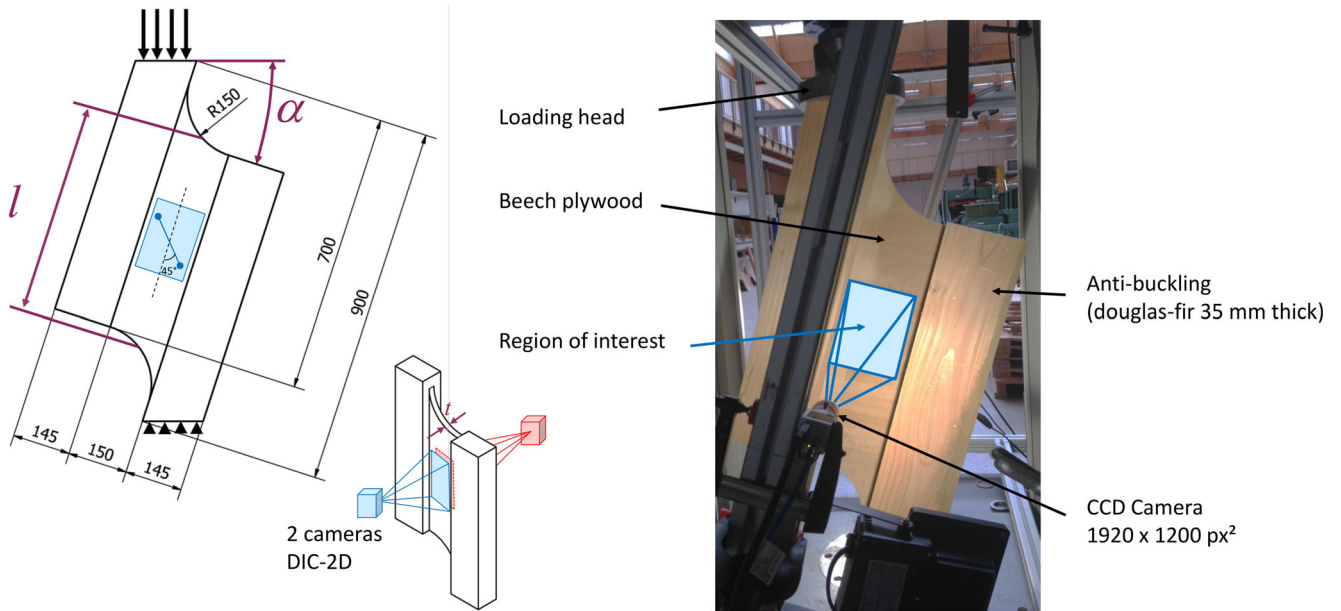


**Fig. 2** Experimental test setup

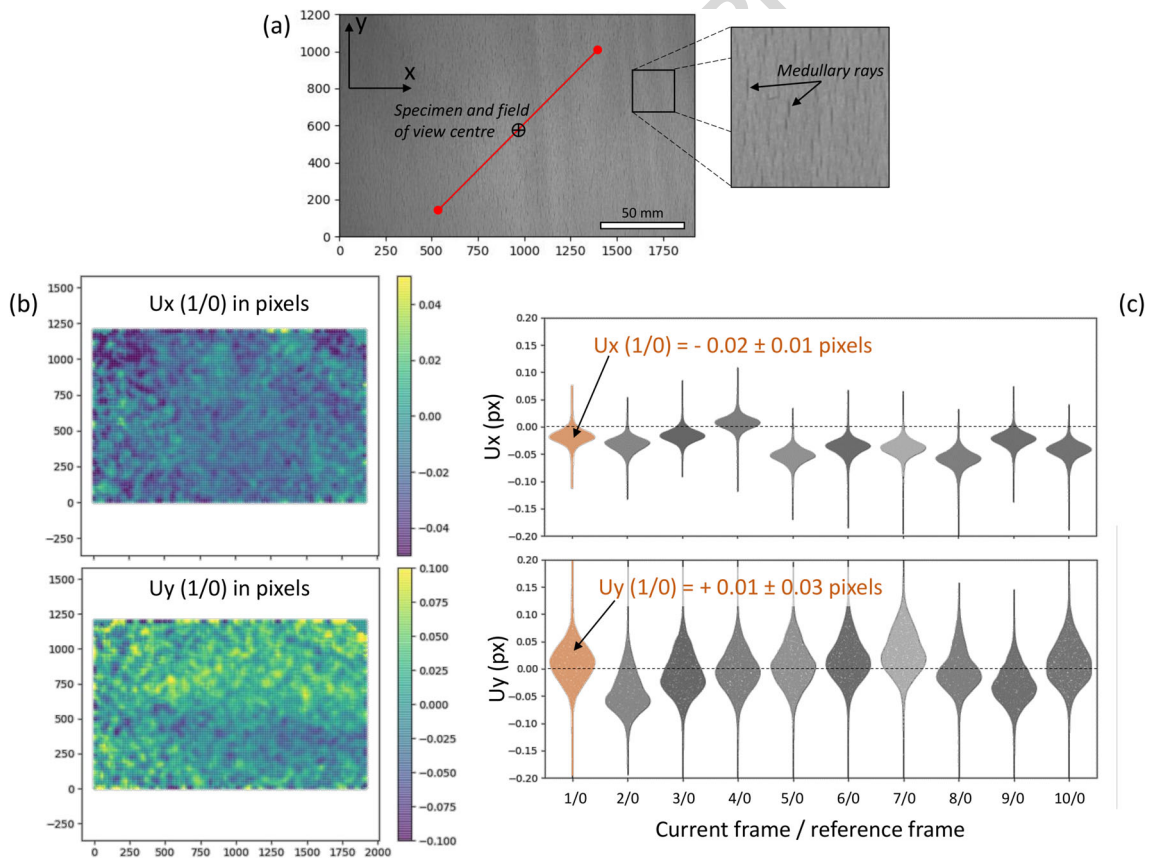


**Fig. 3** **a** beech natural pattern for DIC on one sample showing medullary rays (elliptical darker shapes), **b** corresponding X-and Y-displacement fields obtained between the first image and the reference image, **c** DIC pseudostatic accuracy assessment from 10 consecutive images taken free from loading

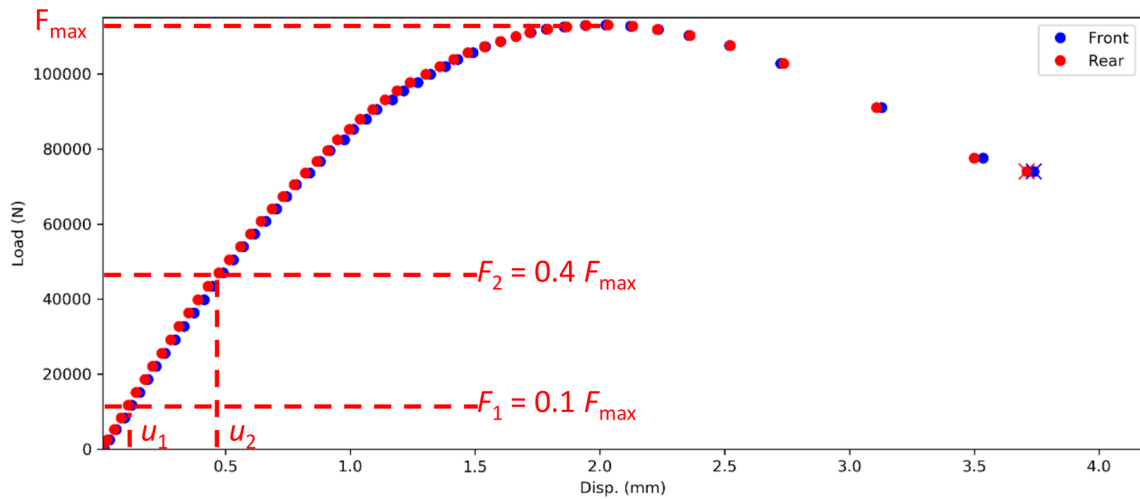


Fig. 4 Typical load-displacement curves (front and rear) used for the panel shear properties assessments. The displacement represents the distance measured by DIC between two points located on the compression diagonal at 45° to the rails passing through the centre of the shear area

104 precisely on both sides of the specimen and centred on  
 105 both camera respective fields of view before tests were  
 106 performed (see Fig. 3(a)). Moreover, the alignment of the  
 107 camera axis with the specimen ones, as represented in the  
 108 Fig. 2, was ensured by imposing their correspondence with  
 109 the anti-buckling beams, and the camera orientation (sensor  
 110 parallel with the observed area) was checked using a grid  
 111 calibration plate. The magnification factor obtained with  
 112 such experimental set up was 9.08 px/mm (or 0.11 mm/px).  
 113 Hardware and software resources have been developed  
 114 specifically to record simultaneously the load value and  
 115 its corresponding pictures. The experimental test setup is  
 116 described in Fig. 2.

117 The principle of Digital Image Correlation is to compare  
 118 digitized images of non-deformed specimen (reference) to  
 119 multiple images of the same specimen while applying the  
 120 loading to obtain the full-field displacement. An important  
 121 element of the measurement procedure is the image analysis  
 122 software package which is supposed to provide an apparent  
 123 2-D displacement field that maps a so-called "reference  
 124 image" to a "deformed image" at a discrete set of positions,  
 125 according to the principle of optical flow conservation.  
 126 The displacement was computed using the image analysis  
 127 software, DaVIS 10.0.5, by LaVision. In the case of this

128 study, no surface preparation of the observed area has been  
 129 done, the medullary rays of beech as shown in (Fig. 3(b))  
 130 have been directly used as the pattern from which to  
 131 correlate the images between two successive loading steps.  
 132 The subsize and the stepsize have been taken equal to 51  
 133 and 17 pixels respectively. The region of interest is shown in  
 134 Fig. 2. The image acquisition frequency was fixed at 0.2 Hz.

135 The natural pattern the beech plywood featured, see  
 136 (Fig. 3(a)), appeared as really satisfying among the different  
 137 surface preparation considering the difficulty to master the  
 138 paint application on big amount of samples compared to  
 139 the accuracy required for the shear modulus determination  
 140 (some details regarding this will be discussed in Section  
 141 "Mechanical Properties Calculation"). Nonetheless, the  
 142 natural pattern of beech veneer is anisotropic due to  
 143 the presence of elliptic and oriented medullary rays  
 144 affecting the correlation error which becomes anisotropic  
 145 correspondingly.

Table 1 Material properties used in finite elements analysis

Property	Ply material (beech) [20]	Wood support (Douglas fir) [21]
$E_X$ (MPa)	14000	14740
$E_Y$ (MPa)	1160	737
$\nu_{XY}$	0.45	0.45
$G_{XY}$ (MPa)	1080	1150

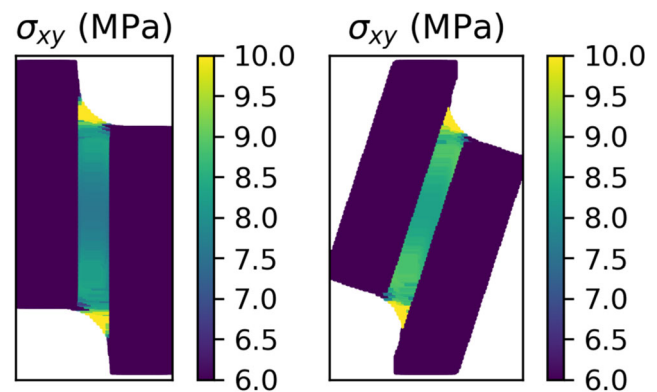
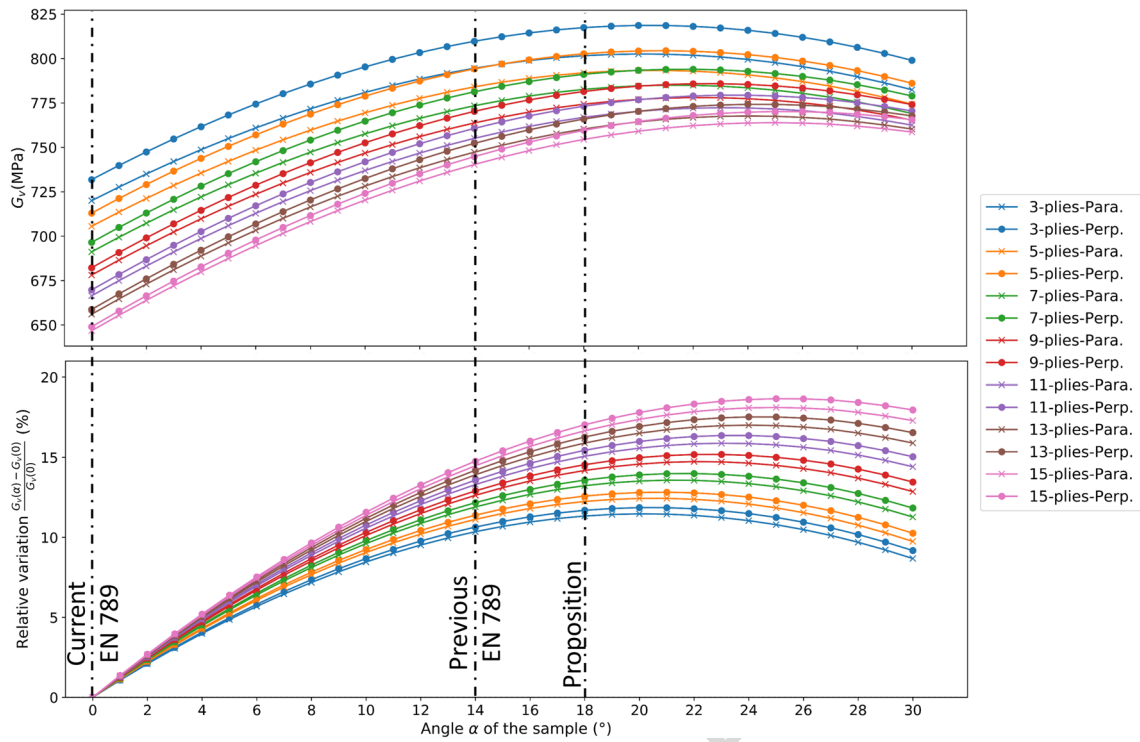


Fig. 5 Comparison of the modeled strain field obtained from vertical and titled samples





**Fig. 6** Influence of tilting the sample at different angle on the calculation of  $G_v$ . The results for two types of sample (Parallel and Perpendicular) and different thicknesses are presented. The upper part shows the calculated  $G_v$  and the lower part the relative variation observed with the configuration without tilting the sample

146 The average correlation error is determined using the  
 147 10 images taken before the loading is applied for each  
 148 sample, performing a DIC computation on them under the  
 149 exact same calculation settings (subset size 51 pixels and  
 150 step size 17 pixels), and extracting the standard deviation  
 151 at 68% confidence interval of the X- and Y-displacement  
 152 fields obtained for those non-deformed configurations. An  
 153 example is provided in (Fig. 3(b)). Thus, the average  
 154 displacement field error, arising from the whole samples  
 155 batch on both sides, were  $\pm 4.4E^{-3}$  mm ( $\pm 0.02$  pixel)  
 156 and  $\pm 2.2E^{-3}$  mm ( $\pm 0.01$  pixel) respectively for the  
 157 medullary rays direction and its normal one displayed by  
 158 (Fig. 3(b) and (c)). Those values embed the pattern quality,  
 159 the enlightenment intensity variations and the eventual  
 160 whole system vibrations (rigid body displacement between  
 161 the sample and the cameras). The influence of this error on  
 162 the calculation of the shear modulus will be discussed later.

### 163 Mechanical Properties Calculation

164 The calculation of the shear modulus is based on  
 165 load-displacement curves. The displacement is measured  
 166 between two selected positions on the images. Those two  
 167 positions were located on the compression diagonal at  $45^\circ$   
 168 to the rails passing through the centre of the shear area. The  
 169 distance between the two points is equal to 120 mm and

170 corresponds to the theoretical position of the extensometer  
 171 prescribed in EN 789 [7] (see Fig. 2).

172 The invasive attachment of a physical extensometer with  
 173 pins inserted in holes is not necessary thanks to the use of  
 174 DIC. An example on a load-displacement curves obtained  
 175 on the two faces of the sample is described in Fig. 4. The  
 176 section of the graph between  $0.1F_{max}$  and  $0.4F_{max}$  is  
 177 used for a linear regression analyses and the panel shear  
 178 modulus of rigidity is then calculated using (equation (1)).  
 179 This equation is similar to the one given in the standard  
 180 except for the  $\cos(\alpha)$  term introduced to take into account  
 181 the tilting angle [7].

$$G_v = \frac{0.5\cos(\alpha)(F_2 - F_1)l_1}{(u_2 - u_1)lt} \quad (1)$$

182 where:

- 183 –  $(F_2 - F_1)$  is the increment of load between  $0.1F_{max}$  and  
 184  $0.4F_{max}$  in N,
- 185 –  $(u_2 - u_1)$  is the increment of deflection corresponding  
 186 to  $(F_2 - F_1)$  using a linear regression in mm,
- 187 –  $l_1$  is the distance between the two selected points and is  
 188 equal to 120 mm,
- 189 –  $l$  is the length of the test piece measured along the centre  
 190 line of the shear area (including the radius section) in  
 191 mm,

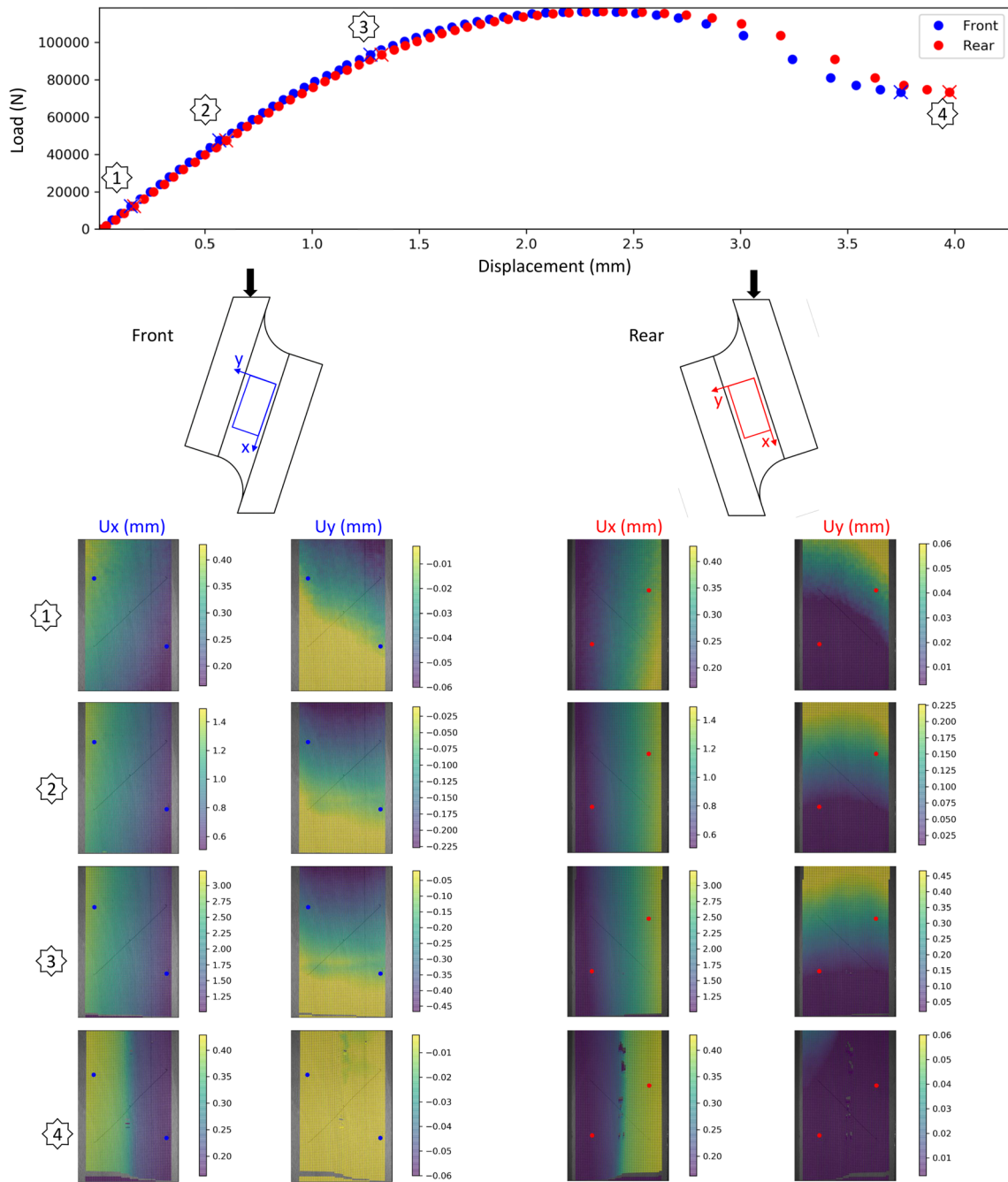


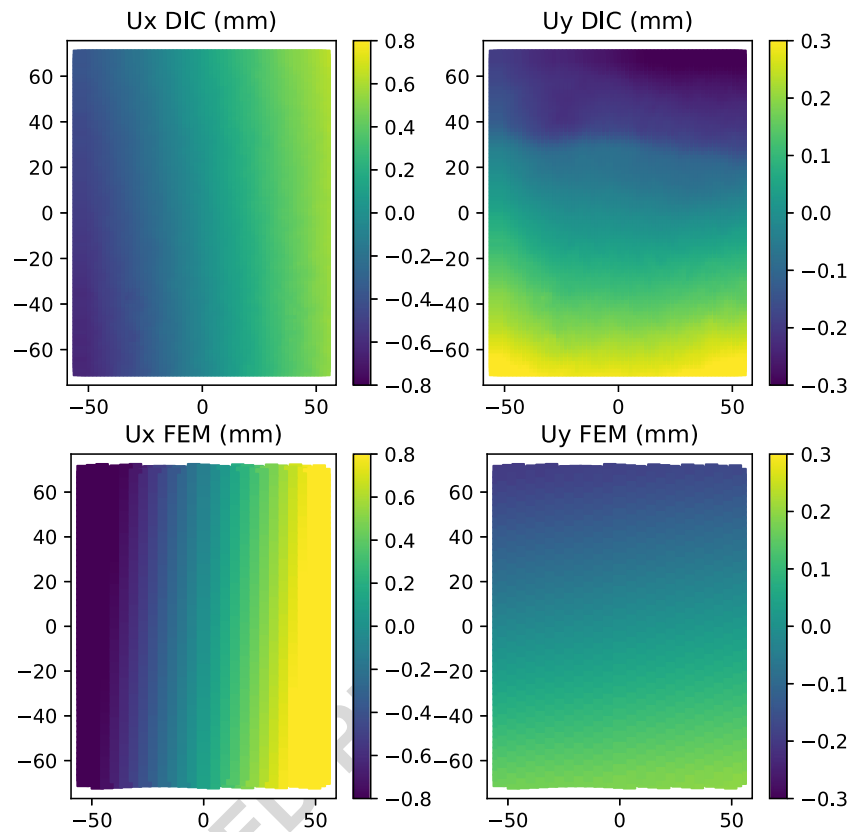
Fig. 7 Typical results of a shear test. The upper part represents the load-displacement curve during the test. Four levels of solicitation are highlighted and their respective displacement fields for both sample sides and two directions are presented in the lower part

192 –  $t$  is the average thickness of the test piece measured at  
 193 two points along the centre line of the shear area in mm,  
 194 –  $\alpha$  is the tilting angle of the sample in  $^{\circ}$ .

195 An analysis of the error sources to determine the shear  
 196 modulus  $G_v$  from (equation (1)) leads to a relative error on

197 the shear modulus of 1.4 % with the following individual 197  
 198 error (experimentally determined or from device calibration 198  
 199 certificates):  $\Delta\alpha = \pm 1^{\circ}$ ;  $\Delta F = \pm 0.5\% F = \pm 344$  N; 199  
 200  $\Delta u = \pm 4.9E-3$  mm;  $\Delta l_1 = \pm 0.5$  mm;  $\Delta l = \pm 1$  mm;  $\Delta t$  200  
 201  $= \pm 0.01$  mm. This determined  $G_v$  error is mostly affected 201  
 202 by the displacement one but remains very low, sustaining 202

**Fig. 8** Comparison of displacements fields obtained on the front side experimentally by DIC and numerically by FEM



203 the applicability of DIC method using directly the natural  
 204 beech wood aspect (medullary rays) as pattern (no surface  
 205 preparation as paint speckle needed).

206 The panel shear strength is calculated from (equation (2))  
 207 where  $F_{max}$  is the maximum load applied up to failure. In this  
 208 case too the equation only differs by the  $\cos(\alpha)$  term [7].

$$f_v = \frac{F_{max} \cos(\alpha)}{lt} \quad (2)$$

209 **Numerical Model**

210 To evaluate the influence of the test modification, a  
 211 model has been developed using quadratic triangular  
 212 elements (6-nodes) with orthotropic material properties.  
 213 The finite element solver used for this study is CAST3M  
 214 2019 [19], the mechanical software developed by the  
 215 CEA (French Atomic Energy and Alternative Energies  
 216 Commission). The grain directions between the different  
 217 plies were alternatively  $0^\circ$  and  $90^\circ$  to fit with plywood  
 218 panel composition. The performed simulations were linear  
 219 regarding the material properties and deflections. The  
 220 boundary conditions were as follows: for the lower support,  
 221 displacements were locked in both directions (X and Y),  
 222 and in the upper support displacements were locked in  
 223 horizontal direction (X). The tilting angle of the sample  
 224 varies between  $0^\circ$  and  $30^\circ$ , and the number of plies  
 225 varies between 3 and 15. The thickness of each ply has been

226 taken equal to 2 mm. The material properties used in the  
 227 calculations are shown in Table 1 and were taken from the  
 228 literature [20, 21]. X and Y directions being respectively the  
 229 fiber direction and the direction perpendicular to the fiber.  
 230 Given the purpose of the model, the interface between the  
 231 plies is not modeled.

232 In addition, two types of specimens were modeled in  
 233 a similar way to the normative recommendations: test  
 234 specimens with their face grain angle oriented parallel to  
 235 the load (called type Parallel), and specimens with their face  
 236 grain angle oriented perpendicular to the load (called type  
 237 Perpendicular).

238 **Results and Discussions**

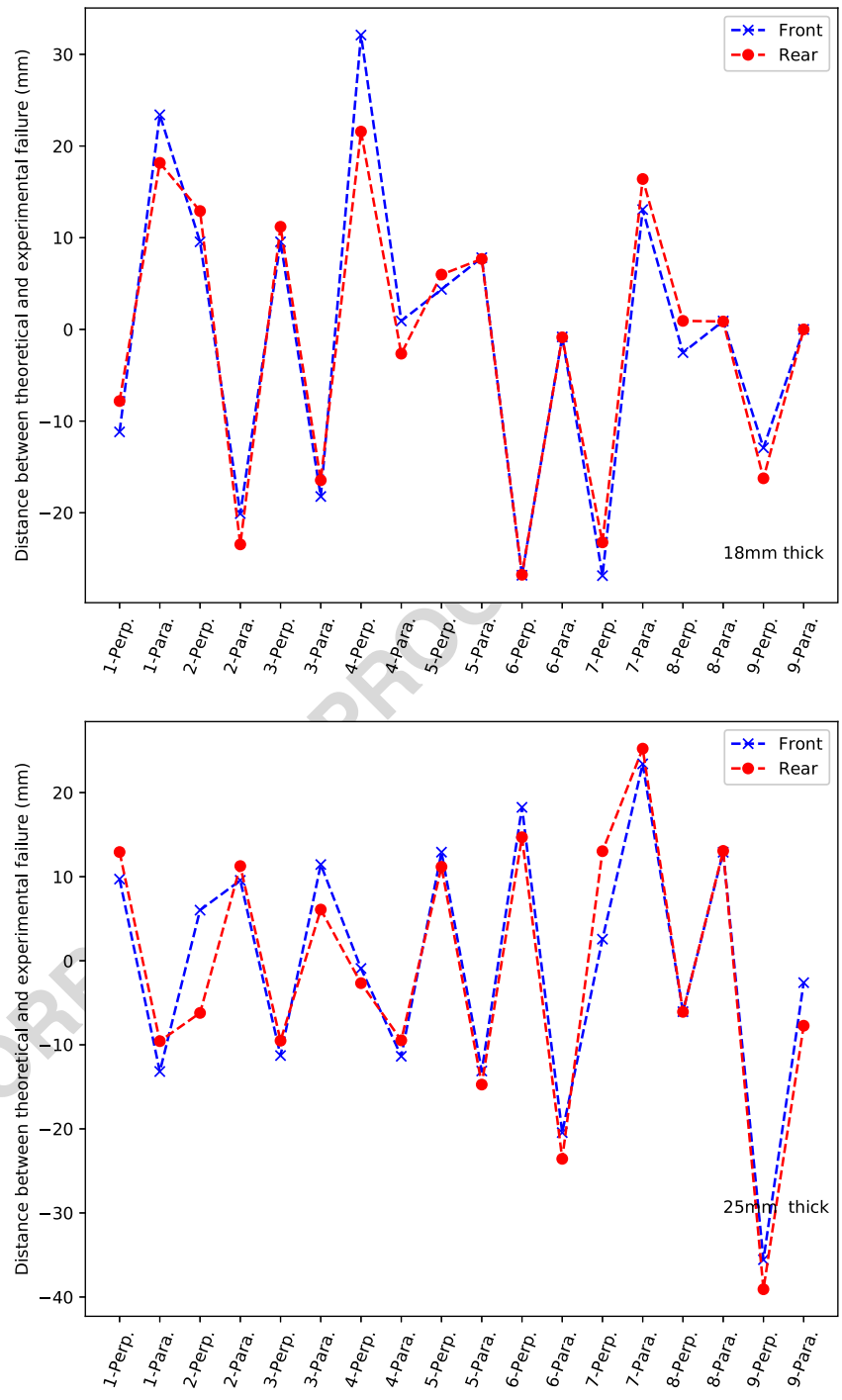
239 **Results of the Numerical Model**

240 The comparison of the shear stress fields, for the same  
 241 displacement of the loading head, obtained thanks to the  
 242 FEM after tilting the sample is given in Fig. 5. The different  
 243 fields were really close to each other either quantitatively  
 244 or qualitatively. The shear stress in the middle part of the  
 245 sample is nearly constant in both cases and validate the  
 246 sample tilting strategy.

247 The shear modulus of rigidity calculated for each  
 248 simulation is presented in Fig. 6. As one of the model



**Fig. 9** Distance between the failure position identified using DIC and the geometric centre of the sample. The upper part is related to 18 mm thick samples and the lower part show the results for 25 mm thick samples



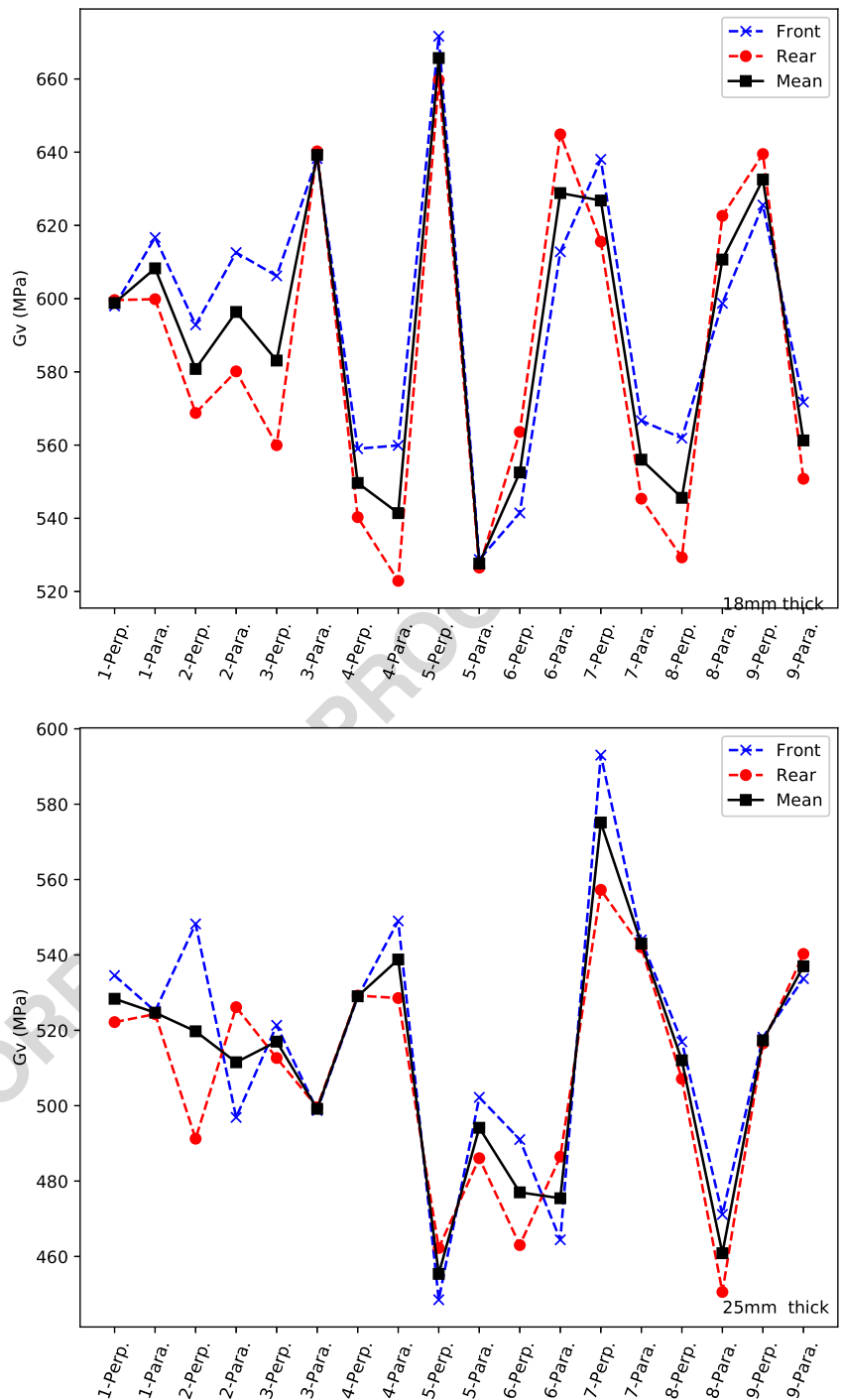
249 outcomes, it can be seen that the sample type Perpendicular  
 250 has a higher shear modulus than the Parallel type. The  
 251 difference observed between the sample types is higher for  
 252 panels with a lower number of plies. These results highlight  
 253 the homogenization process that occurs by increasing the  
 254 number of plies. The shear modulus of rigidity is lower as  
 255 the number of plies increases. The modeled shear modulus  
 256 is increasing as the angle of the sample increases until

it reaches a maximum value (from 20° to 26° depending  
 on the number of plies), then it decreases as the angle  
 continues to increase. The relative variation of the shear  
 modulus of rigidity for several tilting angles compared to  
 the simulation with the non tilted configuration ( $\alpha = 0^\circ$ ) is  
 presented in Fig. 6. The variation is inferior to 20% in every  
 cases. As the number of plies increases the relative variation  
 also increases. The relative variation for an angle of 18°

257  
 258  
 259  
 260  
 261  
 262  
 263  
 264



**Fig. 10** Comparison of the shear modulus calculated on both side of the sample. The upper part is related to 18 mm thick samples and the lower part shows the results for 25 mm thick samples



265 is comprised between 11% and 17% for every modeled  
 266 cases. This value has to be compared to a relative variation  
 267 comprised between 10% and 15% for an angle equal to 14°  
 268 as it was in the previous standard EN 789 (Fig. 1(b)).

**Displacement Field and Shear Solicitation**

The typical results obtained for a single test are presented in Fig. 7 (18 mm thick and Parallel type panel). The load-

269  
 270  
 271



**Table 2** Minimum, mean, maximum, 5% percentiles values, standard deviations and coefficient of variation for different characterized properties

	Min	5% quant.	Mean	Max	SD	CV (%)
Density (kg.m <sup>-3</sup> )						
18 mm thick.	661.9	682.4	717.7	752.2	18.3	2.5
Para.	699.7	695.5	720.7	741.2	11.9	1.6
Perp.	661.9	664.8	714.8	752.2	23.4	3.3
25 mm thick.	699.9	699.8	729.8	755.3	15.5	2.1
Para.	702.9	695.9	731.2	755.3	16.6	2.3
Perp.	699.9	695.9	728.5	746.9	15.3	2.1
All samples	661.9	690.9	723.8	755.3	17.8	2.5
$G_v$ (MPa)						
18 mm thick.	520.8	506.2	587.6	665.7	42.1	7.2
Para.	527.6	500.4	585.5	639.2	40.0	6.8
Perp.	520.8	490.7	589.6	665.7	46.5	7.9
25 mm thick.	455.4	452.7	512.0	575.1	30.7	6.0
Para.	455.4	428.5	498.2	543.0	32.8	6.6
Perp.	494.1	478.2	525.7	575.1	22.4	4.3
All samples	455.4	452.5	549.8	665.7	52.8	9.6
$f_v$ (MPa)						
18 mm thick.	10.5	10.5	12.0	13.1	0.7	6.1
Para.	10.5	10.1	11.8	12.9	0.8	6.7
Perp.	11.0	10.7	12.1	13.1	0.7	5.6
25 mm thick.	10.0	10.1	11.6	12.8	0.8	7.0
Para.	10.0	9.6	11.5	12.4	0.9	7.7
Perp.	10.8	10.2	11.8	12.8	0.7	6.2
All samples	10.0	10.4	11.8	13.1	0.8	6.6

272 displacement curves are presented in the upper part. The  
 273 displacement represents the relative displacement of the two  
 274 points as it was described before in the Section “**Mechanical**  
 275 **Properties Calculation**” for each side of the panel (front and  
 276 rear) analogously to the method described in EN 789. The  
 277 two selected points are also visible on the displacements  
 278 fields. The different steps for which displacements field  
 279 are plotted correspond respectively to results under a load  
 280 equal to  $0.1 F_{max}$ ,  $0.4 F_{max}$ ,  $0.8 F_{max}$  and after failure under a  
 281 residual load equal to  $0.63 F_{max}$ . For each step displacement  
 282 fields in x-direction for both sides (Ux Front and Ux  
 283 Rear) and in y-direction (Uy Front and Uy Rear) are  
 284 presented. The measured displacement on both sides were  
 285 really close to each other. This result can be seen on the  
 286 load-displacement curve as well as on the displacement  
 287 fields.

288 One of the advantages of DIC is that it allows to check  
 289 the validity of the solicitation. The comparison of the  
 290 displacements fields obtained on the front side by DIC and  
 291 by FEM is presented in Fig. 8. The comparison is made at  
 292 the same load and corresponds to the third step described  
 293 previously (i.e at  $0.8 F_{max}$ ). The comparison is done on the

294 displacements fields where the rigid body motion had been  
 295 removed. It can be seen that the displacements fields in both  
 296 directions were similar quantitatively.

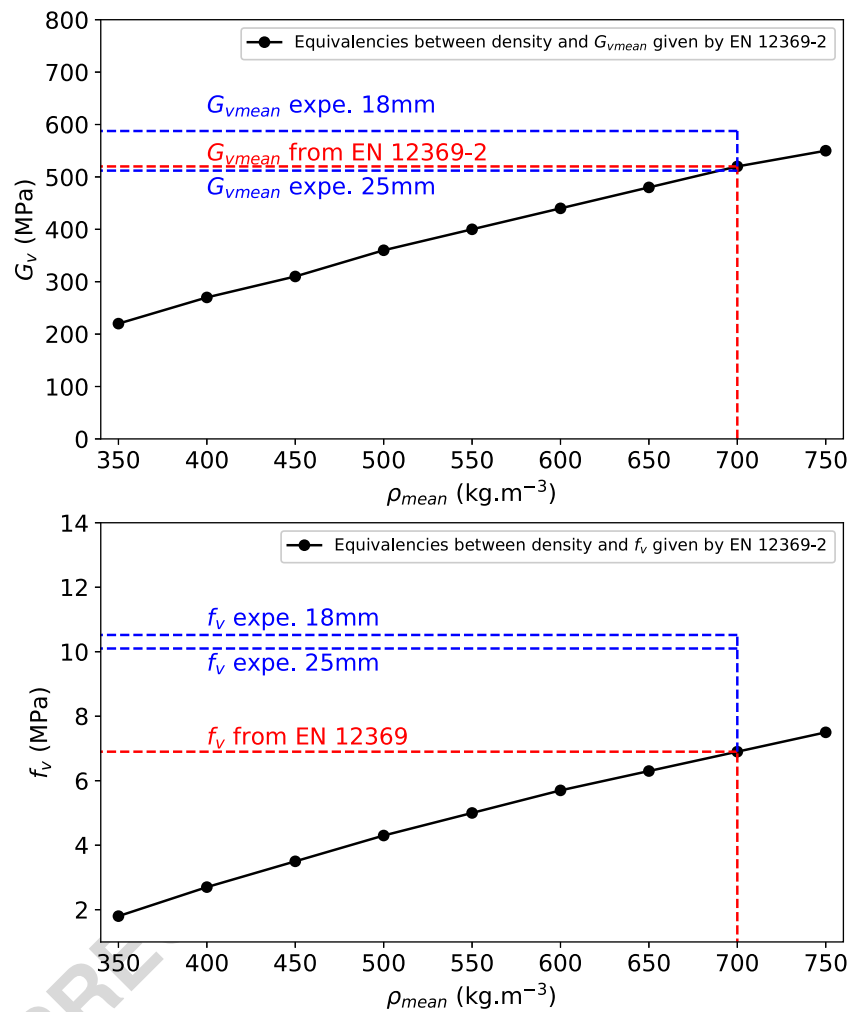
297 The lower part of Fig. 7 shows that this method is an  
 298 effective way to identify the failure position. The failure  
 299 position computed on the two sides of every samples is  
 300 presented in Fig. 9. The distance from the centre and  
 301 the actual failure path is comprised between -39.1 and  
 302 32.1 mm. Therefore, every sample has been accepted for  
 303 the computation of the shear strength since no failure  
 304 occurred in another way than in shear between the two  
 305 rails. The average absolute distance between the failure  
 306 and the geometric centre is equal to 12.4 mm which can  
 307 be considered low enough to use the shear length  $l$  in the  
 308 calculation of the shear strength.

**Mechanical Properties Analysis** 309

310 Figure 10 presents the results of the shear modulus for  
 311 the 36 panels, the upper part for the 18 mm thick panels  
 312 and the lower part for the 25 mm thick panels. The blue  
 313 dashed line represents the shear modulus calculated on the



**Fig. 11** Comparison between experimental values and equivalencies given in EN 12369-2



314 basis of the DIC measurement on the front side, the red  
 315 dashed line the one measured on the rear side, and the black  
 316 plain line their mean value. Those results show that the  
 317 difference between the shear modulus calculated on both  
 318 sides is low. Indeed, the mean relative variation is equal to  
 319 only 3.6% with a maximal relative variation equal to 13.7%.  
 320 These percentages represent a mean absolute variation of  
 321 20.2 MPa and a maximal variation of 76.5 MPa on the shear  
 322 modulus.

323 Descriptive statistics for the density, the shear modulus,  
 324 and the shear strength are given in Table 2. The mean value  
 325 for 18 mm thick and 25 mm thick panel were respectively  
 326 equal to 717.7 and 729.8 kg·m<sup>-3</sup>. The corresponding  
 327 coefficients of variation were equal to 2.5 and 2.1% which  
 328 is consistent with the literature in the case of beech [22–  
 329 25]. The mean shear modulus G<sub>v</sub> is respectively equal to  
 330 587.6 and 512.0 MPa for 18 and 25 mm thick samples. This  
 331 result is consistent with the results based on the numerical  
 332 model. In addition, the samples from the type Perp. have  
 333 a higher shear modulus in every case which is also in  
 334 accordance with the numerical model. Finally, the average

335 shear strength f<sub>v</sub> and its corresponding variability were  
 336 really close for every thicknesses and sample types; the  
 337 global averaged shear strength is approximately equal to  
 338 12 MPa.

**Interest of the Test Realization Over Density Based  
 Equivalencies**

341 The survey conducted on the plywood panel manufacturers’  
 342 performances reports in Europe revealed that the majority  
 343 of producers use density-based equivalencies given by the  
 344 standards [8] to provide shear properties. The average  
 345 densities for 18 mm and 25 mm thick panels were  
 346 respectively 717 and 729 kg·m<sup>-3</sup>, according to the same  
 347 standard the value of 700 kg·m<sup>-3</sup> must be used (N.B.:  
 348 its lower limit must be used). Using this threshold, the  
 349 shear properties could be taken equal to 520 and 6.9 MPa  
 350 for the shear modulus and the shear strength respectively.  
 351 Figure 11 presents the comparison between values obtained  
 352 experimentally in this study and the values taken from the  
 353 equivalencies applying the standards. These results show

354 that the realization of the shear tests is favorable or at least  
355 equivalent in the case of the shear modulus and always  
356 favorable for the calculation of the shear strength.

## 357 Conclusion

358 This study proposed a modified of the two rails shear test  
359 in a more functional configuration, meaning without the  
360 use of a bulky apparatus. The validity of the tests has  
361 been shown by the use of full field measurement using  
362 DIC. Nevertheless, the test could still be performed using a  
363 simpler measurement device such as a LVDT in the tilted  
364 proposed configuration. The interest of the realization of  
365 these tests has been highlighted in comparison with the use  
366 of equivalences based on the measurement of the average  
367 density. In any case, the measurements taken from the tests  
368 can lead to the declaration of shear properties equivalent  
369 or even greater than those expected by the standard  
370 and thus enhance significantly the valorization of beech  
371 plywood.

372 **Acknowledgements** The present study was financed by the company  
373 Fernand BRUGERE. This study was performed thanks to the  
374 partnership build by BOPLI: a shared public-private laboratory  
375 build between Bourgogne Franche-Compté region, LaBoMaP and the  
376 company Fernand BRUGERE. The authors would also like to thank  
377 the Xylomat Technical Platform from the Xylomat Scientific Network  
378 funded by ANR-10-EQPX-16 XYLOFOREST.

## 379 Compliance with Ethical Standards

380 **Conflict of interests** The authors declare that they have no conflict of  
381 interest.

## 382 References

- 383 1. Dobbin McNatt J (1969) Rail shear test for evaluating edgewise  
384 shear properties of wood base panel products. tech. rep., U.S.D.A  
385 Forest Service, Forest Products Laboratory. Madison
- 386 2. Munthe B, Ethington RL (1968) Method for evaluating shear  
387 properties of wood. US Department of Agriculture, Forest Service,  
388 Forest Products Laboratory
- 389 3. Rune Z (1994) Evaluation Of test methods for wood based panels.  
390 Determination of shear modulus and shear strength. Tech. Rep.  
391 Nordtest Project No. 1060–92, Swedish National Testing and  
392 Research Institute
- 393 4. Ehlbeck J, Colling F (1984) Determination of panel shear  
394 strength and shear modulus of beech plywood in structural sizes.  
395 (SWITZERLAND)
- 396 5. Wilson CR, Parasin AV (1979) A comparison of plywood modulus  
397 of rigidity determined by the ASTM and RILEM/CIB-3tt test  
398 methods. (Austria)
- 399 6. Booth LG, Kuipers J, Noren B, Wilson CR (1977) Methods of  
400 test for the determination of mechanical properties of plywood,  
401 (Sweden)
- 402 7. CEN (2005) EN 789 timber structures - test methods -  
403 determination of mechanical properties of wood based panels

8. CEN (2011) EN 12369-2 wood-based panels - characteristic 404  
values for structural design - Part 2: Plywood 405
9. Yoshihara H, Yoshinobu M (2015) Young's modulus and shear 406  
modulus of solid wood measured by the flexural vibration 407  
test of specimens with large height/length ratios. *Holzforschung* 408  
69(4):493–499 409
10. Cavalli A, Marcon B, Cibecchini D, Mazzanti P, Fioravanti M, 410  
Procino L, Togni M (2017) Dynamic excitation and FE analysis 411  
to assess the shear modulus of structural timber. *Mater Struct* 412  
50(2):130 413
11. Vacher P, Dumoulin S, Morestin F, Mguil-Touchal S (1999) 414  
Bidimensional strain measurement using digital images. *Proc Inst* 415  
*Mech Eng C J Mech Eng Sci* 213(8):811–817 416
12. Wattrisse B, Chrysochoos A, Muracciole J-M, Némoz-Gaillard M 417  
(2001) Analysis of strain localization during tensile tests by digital 418  
image correlation. *Exp Mech* 41(1):29–39 419
13. Sutton M, Wolters W, Peters W, Ranson W, McNeill S 420  
(1983) Determination of displacements using an improved 421  
digital correlation method. *Image Vis Comput* 1(3):133– 422  
139 423
14. Bruck H, McNeill S, Sutton MA, Peters W (1989) Digital image 424  
correlation using newton-Raphson method of partial differential 425  
correction. *Exp Mech* 29(3):261–267 426
15. Bornert M, Brémand F, Doumalin P, Dupré J-C, Fazzini M, 427  
Grédiac M, Hild F, Mistou S, Molimard J, Orteu J-J, Robert L, 428  
Surrel Y, Vacher P, Wattrisse B (2009) Assessment of digital 429  
image correlation measurement errors: methodology and results. 430  
*Exp Mech* 49(3):353–370 431
16. Jeong GY, Zink-Sharp A, Hindman DP (2009) Tensile properties 432  
of earlywood and latewood from loblolly pine (*Pinus taeda*) 433  
using digital image correlation. *Wood Fiber Sci* 41(1):51– 434  
63 435
17. Zink AG, Davidson RW, Hanna RB (2007) Strain measurement in 436  
wood using a digital image correlation technique. *Wood Fiber Sci* 437  
27(4):346–359 438
18. Haldar S, Gheewala N, Grande-Allen K, Sutton M, Bruck 439  
H (2011) Multi-scale mechanical characterization of palmetto 440  
wood using digital image correlation to develop a template for 441  
biologically-inspired polymer composites. *Exp Mech* 51(4):575– 442  
589 443
19. CEA (2019) Cast3m 444
20. Guitard D (1987) Mécanique du matériau bois et composites. 445  
NABLA, cepadues ed. 446
21. Bergman R, Cai Z, Carll CG, Clausen CA, Dietsberger MA, 447  
Falk RH, Frihart CR, Glass SV, Hunt CG, Ibach RE (2010) Wood 448  
handbook: Wood as an engineering material. Forest Products 449  
Laboratory 450
22. Gérard J, Guibal D, Paradis S, Vernay M, Beauchêne J, 451  
Brancheriau L, Châlon I, Daigremont C, Détienne P, Fouquet D, 452  
Langbour P, Lotte S, Thévenon M-F, Méjean C, Thibaut A (2011) 453  
*Tropix* 7 454
23. Pöhler E, Klingner R, Künniger T (2006) Beech (*Fagus sylvatica* 455  
L.) – Technological properties, adhesion behaviour and colour 456  
stability with and without coatings of the red heartwood. *Annals* 457  
*Forest Sci* 63(2):129–137 458
24. Viguier J, Bourgeay C, Rohumaa A, Pot G, Denaud L (2018) 459  
An innovative method based on grain angle measurement to sort 460  
veneer and predict mechanical properties of beech laminated 461  
veneer lumber. *Constr Build Mater* 181:146–155 462
25. Viguier J, Marcon B, Girardon S, Denaud L (2017) Effect 463  
of forestry management and veneer defects identified by x-ray 464  
analysis on mechanical properties of laminated veneer lumber 465  
beams made of beech. *BioResources* 466

**Publisher's Note** Springer Nature remains neutral with regard to 467  
jurisdictional claims in published maps and institutional affiliations. 468

